Scanning and Transmission Electron-Microscopic Studies on the Lingual Tonsil of the Buffalo (Bubalus bubalis)

Ibrahim Alhaji Girgiri and Pawan Kumar*

Department of Veterinary Anatomy, College of Veterinary Sciences, Lala Lajpat Rai University of Veterinary and Animal Sciences, Hisar-125 004, India

Abstract: The present study examined lingual tonsil of six buffaloes of the local mixed breed by scanning and transmission electron-microscopy to elucidate their ultrastructural features. The lingual tonsil presented folded mucosa having longitudinally oriented folds which were separated by grooves. The surface mucosa showed a squamous arrangement of cells which delineated from the adjacent cells. The surface of these cells at a higher magnification presented the microplicae of different arrangements which were mainly of closed pattern type and resembled fingerprints of humans. The luminal openings of glandular ducts on the free surface presented varying shapes. The transmission electron-microscopy described ultrastructural details of the different strata of the stratified squamous keratinised, non-keratinised and reticular epithelia. The propria-submucosa contain reticular cells, fibroblast, lymphoid cells, plasma cells, granulocytes and interdigitating cells. Few high endothelial venules observed and the cytoplasmic process of these endothelial cells contained small vacuoles equivalent to vesiculo-vacuolar organelles, membrane-bound bodies and vacuolated structures.

Keywords: Lingual tonsil, Microplicae, Vesiculo-vacuolar organelles, Buffalo.

INTRODUCTION

The lingual tonsil at the root of the tongue was a component of Waldeyer's ring and an important site of invasion of microbial pathogens and immune surveillance [1]. The location played a key immune inductive role for the tonsil, which participates as an effector organ of the local mucosal adaptive immune responses [2]. The lining of the tonsils presented an outward epithelium that functionally represented an inductive site where antigens sampled from the surface stimulated cognate naïve T and B lymphocytes [3]. The subepithelial lymphoid compartments consisted of T-cells mainly localized in the extranodular and mantle zones and the B-cells rich germinal centres [4]. Together, these components provided innate, cellular and humoral immunity at the local and systemic levels [5]. The histological and histochemical structure of lingual tonsil of the buffalo has been earlier described [6, 7]. The present study elucidated in detail the ultrastructural features of the lingual tonsil in buffalo with emphasis on different types of epithelia, lymphoid tissue and high endothelial venules.

MATERIALS AND METHODS

Scanning Electron Microscopy

Fresh tissues of the lingual tonsil (approximately 1 cm) were collected from six heads of adult buffaloes (5-6 years of age) of local mixed breed and fixed in 2% glutaraldehyde solution (prepared with 0.1M phosphate buffer, pH 7.4) for 6-8 hours, after thorough washing with chilled 0.1M phosphate buffer (pH 7.4). The tissues were rewashed twice with 0.1M phosphate buffer, and rest of the procedure was conducted at EM Lab., AIRF, JNU, A.I.I.M.S; New Delhi. The tissues were dehydrated using ascending grades of alcohol, critical point dried, mounted on stubs and sputter-coated with gold-palladium. The tissues were viewed at following high electron tension (EHT-20 kV) and working distance (WD-11.5-12 mm) using a scanning electron microscope (Zeiss EVO-40).

Transmission Electron Microscopy

The tissues were primarily fixed in 2.5% glutaraldehyde solution for 6-8 hours and post-fixed in 2% osmium tetraoxide for 1 hour. The resin blocks were prepared, and thin sections of 1 µ were stained with toluidine blue to select the most appropriate areas of the tissues. The ultrathin sections (50-70 nm) were taken on copper grids, stained with 3% uranyl acetate for 10-15 minutes, followed by 0.4% lead citrate for 5-10 minutes. The stained sections were viewed in a transmission electron microscope (Technai G2, SEI Co.) to record observations.

RESULTS

Scanning Electron Microscopy

The lingual tonsil presented the folded mucosa, which was highly irregular, having the folds present in

*Address correspondence to this author at the Department of Veterinary Anatomy, College of Veterinary Sciences, Lala Lajpat Rai University of Veterinary and Animal Sciences, Hisar-125 004, India; Tel: +919466402637; E-mail: pkumar@luvas.edu.in, pawanrajoria2000@rediffmail.com

ISSN: 1927-5196 / E-ISSN: 1927-520X/20

different directions (Figure **1**). The longitudinal folds were of varying length and width, and these were separated by shallow depressions or the grooves. Each longitudinally-oriented fold presented small corrugations or folds which were narrow, small and transversely oriented. At some places, the folds were not prominent. The higher magnification presented the squamous arrangement of the cells, which mainly delineated from the adjacent cells (Figure **2**). At some places, the desquamating cells also observed. The further higher magnification of the cell surface presented microplicae arranged in different patterns. The majority of the microplicae was of closed type and resembled those of human fingerprints. The microplicae of two adjacent cells did not resemble and were not continuous with each other and generally presented a thicker arrangement at the junction of the two cells (Figure **3**).

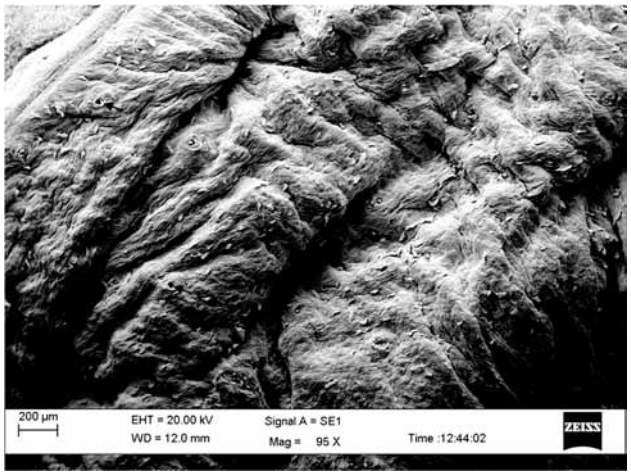

Figure 1: SEM of the surface of the LT showing irregularly arranged folds. Note small openings of glandular ducts (arrow). x 95; (bar 200 µm).

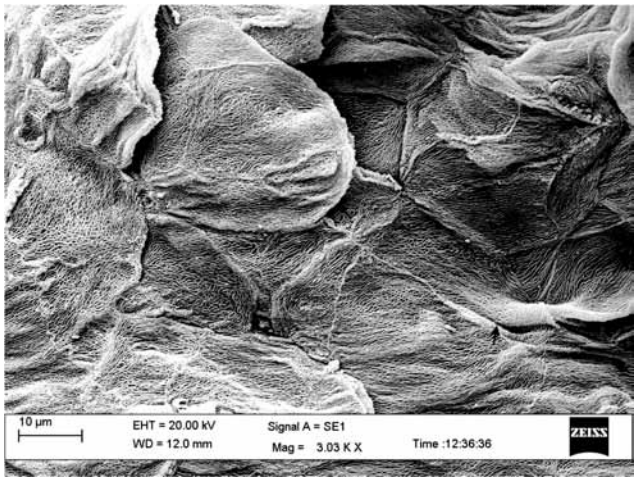

Figure 2: SEM of LT showing squamous arrangement of the cells delineated from the adjacent ones (arrow). x 3003; (bar 10 µm).

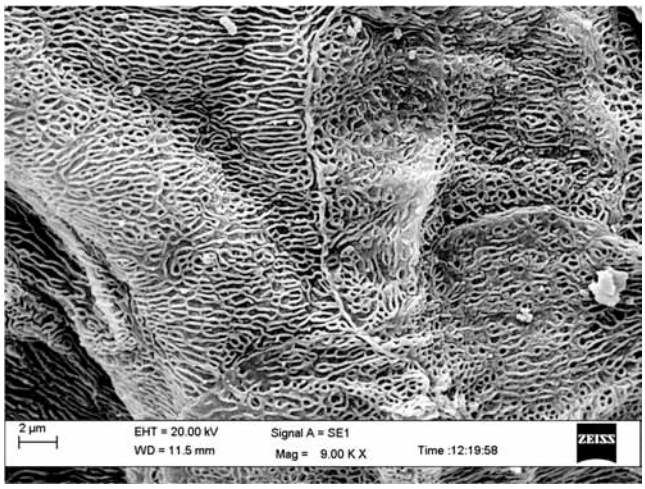

Figure 3: SEM of LT at higher magnification showing varying patterns of microplicae. x 9000; (bar 2 µm).

Small openings of glandular ducts observed irregularly distributed throughout the surface of the lingual tonsil (Figure **1**). These ducts openings were round to oval in shape and presented different arrangement towards their lumen. Some of the ducts presented a flower-like arrangement, whereas some others presented a valve-like arrangement (Figures **4** and **5**). Generally, these duct openings had a narrow rim having the cells arranged in an overlapping pattern. The microplicae were not distinct in the cells lining the lumen of the ducts, rather small microvilli like arrangements were observed.

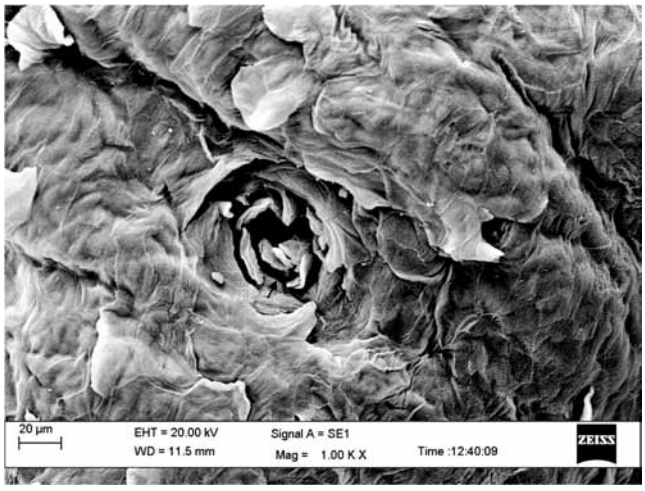

Figure 4: SEM of LT showing flower-like arrangement (arrow) towards lumen of the glandular duct. x 1000; (bar 20 µm).

Transmission Electron Microscopy

The lingual tonsil was lined by stratified squamous keratinized epithelium towards the outer surface. The stratum basale had columnar cells with oval to elongated electron-dense nuclei oriented perpendicular

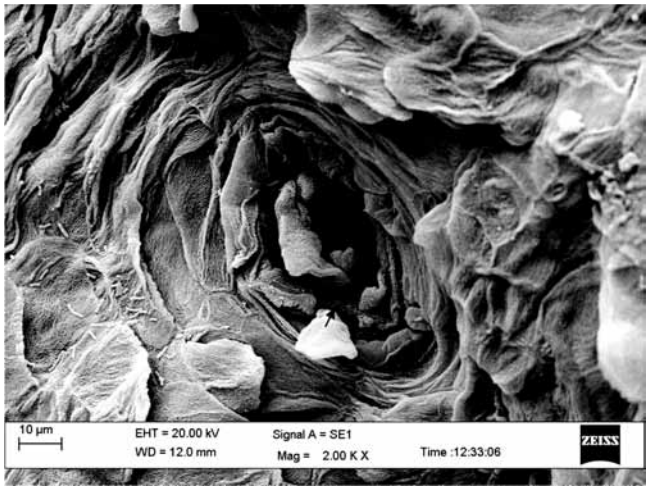

Figure 5: SEM of LT showing valve-like arrangement (arrow) towards opening of the duct. x 2000; (bar 10 µm).

to the length of the epithelium (Figures **6** and **7**). The chromatin material aggregated into smaller clumps and the nucleoli were one to two and centric/eccentric in position. The electron-dense cytoplasm was having mitochondria, Golgi apparatus, endoplasmic reticulum and a few filaments. The adjacent cells of the stratum basale were attached through several desmosomes. The intercellular spaces presented small microvilli-like projections of the cells. A few lymphocytes were seen occasionally in between the stratum basale cells.

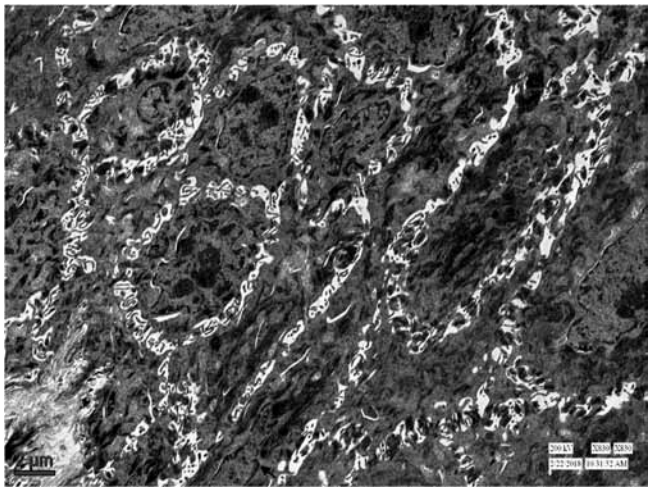

Figure 6: TEM of the LT showing tall columnar shaped cells (arrow) of the stratum basale of stratified squamous keratinized epithelium. x 830; (bar 2 µm).

The stratum spinosum had several rows of cells having comparatively electron-lucent nuclei which were of irregular shapes and generally contained one to two nucleoli. The cytoplasm of these cells contained several tonofilaments and comparatively lesser number of cell organelles than those of stratum basale cells. These cells were also attached by several

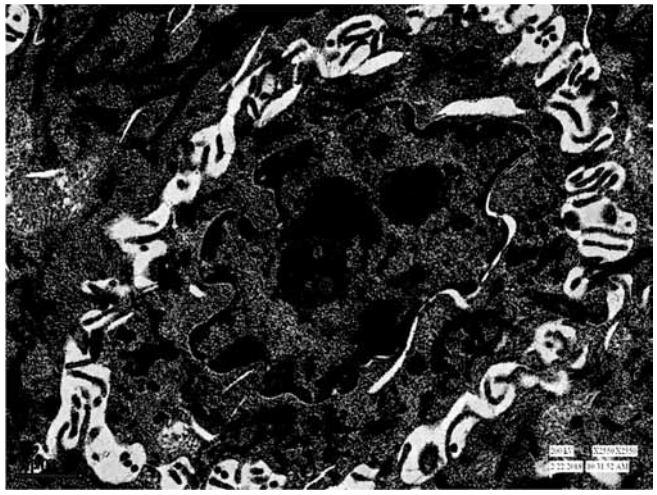

Figure 7: TEM of the LT at a higher magnification showing a cell of the stratum basale of stratified squamous keratinized epithelium. x 2550; (bar 1 µm).

desmosomes, and their interdigitating villi were very closely associated with each other (Figure **8**). The stratum granulosum had horizontally placed electron-lucent nuclei, and their cytoplasm contained few filaments with fewer bundles of tonofilaments, and the cell organelles were further reduced as compared to those of the cells of the stratum spinosum. These cells had extensive processes which were tapering, and the intercellular spaces were reduced, showing interdigitating villi-like projections (Figure **9**).

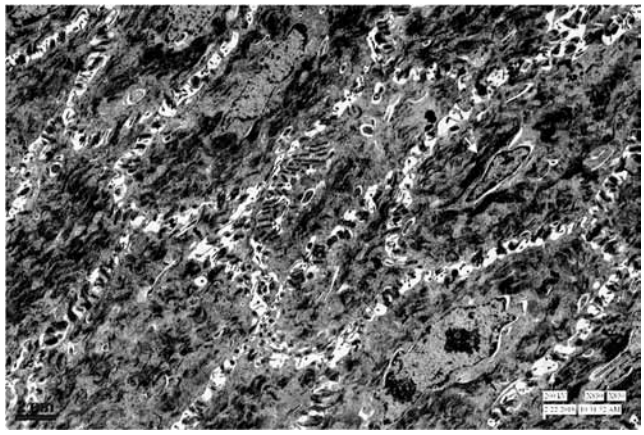

Figure 8: TEM of the LT showing cells of the stratum spinosum (arrow) of stratified squamous keratinized epithelium. x 830; (bar 2 µm).

The stratum corneum was comprised of a mixed population of irregularly shaped electron-lucent and electron-dense cells. The cytoplasm of these cells had fine filaments along with some membrane-bound vesicles and granules. The free surface of these cells presented small spike or spicule-like projections; otherwise, the desquamating cells were also observed (Figure **10**).

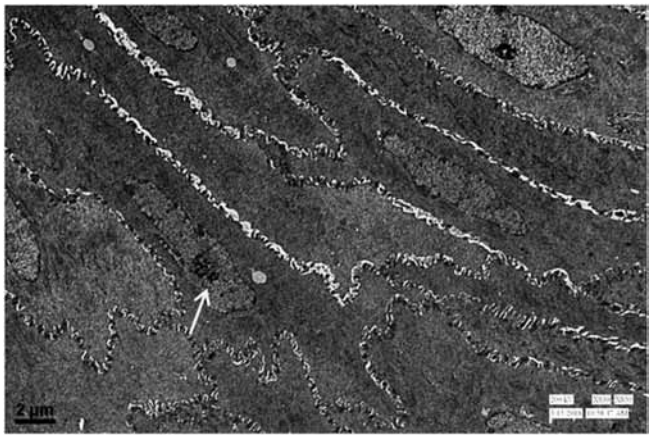

Figure 9: TEM of the LT showing the horizontally placed electron-lucent nuclei (arrow) of cells of the stratum granulosum. x 830; (bar 2 µm).

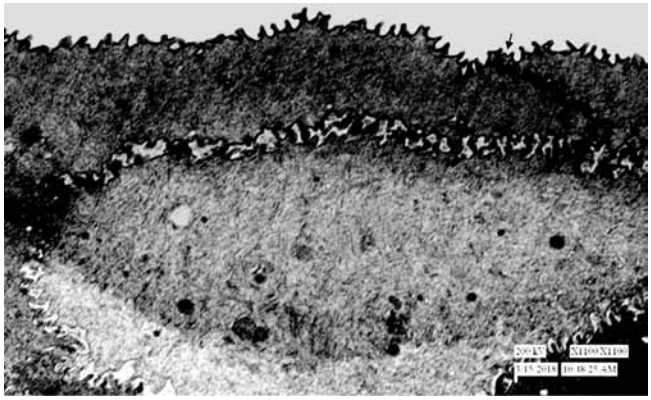

Figure 10: TEM of the LT showing layer of the stratum corneum. Note the spicule-like projection towards the free surface (arrow). x 1100; (bar 2 µm).

The reticular epithelium having stratified squamous non-keratinized epithelium presented features of stratum basale and spinosum similar to those of the surface epithelium. The stratum superficially presented the different types of surface epithelial cells. At places, these were cuboidal whereas at other these were squamous type (Figures **11** and **12**). The nuclei of these cells were electron-lucent and presented smaller aggregations of chromatin towards the nuclear membrane.

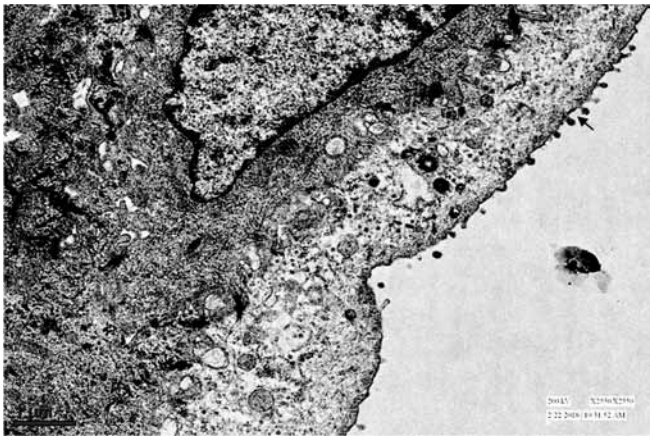

Figure 11: TEM of the LT showing cuboidal type (arrow) of surface epithelial cell of the stratum superficiale of the reticular epithelium. x 2550; (bar 1 µm).

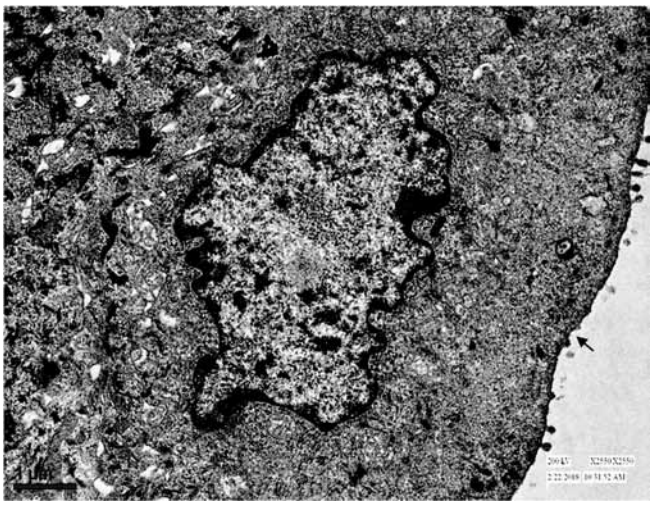

Figure 12: TEM of the LT showing cuboidal type (arrow) of surface epithelial cell of the stratum superficiale of the reticular epithelium. x 2550; (bar 1 µm).

The cytoplasm of these cells presented electron-dense granules, few filaments, a few endoplasmic reticula, and isolated mitochondria.

The free surface of these cells presented very small-sized microvilli-like projections (Figures **11** and **12**). Some of these cells presented more electron-lucent cytoplasm comprising of tonofilaments, multivesicular bodies, cytoplasmic vacuoles, few mitochondria and endoplasmic reticulum.

The propria-submucosa constituted by fine blood capillaries, reticular cells, fibroblast, collagen bundles and lymphoid cells (Figures **13** and **14**). At places, the plasma cells showing typical cartwheel appearance of the nuclei interspersed in between the lymphoid cells. A few granulocytes, especially the neutrophils (Figures **14** and **15**) and a few macrophages showing engulfed material also observed in the subepithelial portion. At some places, the interdigitating cells, fine blood capillaries and pericytes were also observed (Figure **14**).

A few high endothelial venules (HEV'S) also observed. The nuclei of these endothelial cells were irregular shaped, and some of which presented indentations (Figures **16-18**). These nuclei had electron-lucent material except dense chromatin only

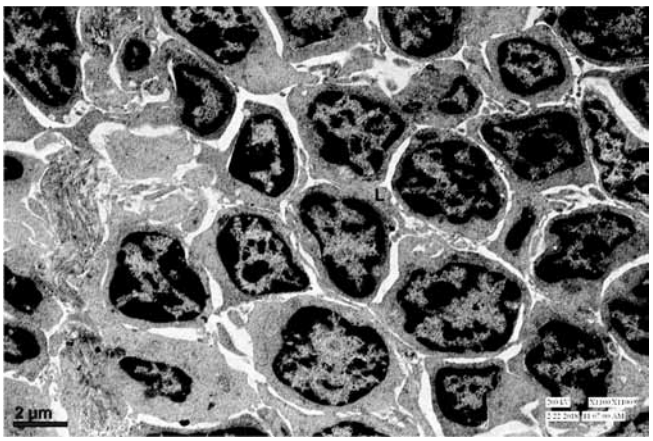

Figure 13: TEM of the LT showing population of lymphoid cells (L) in the propria-submucosa. x 1100; (bar 2 µm).

Figure 14: TEM of the LT showing interdigitating cell (arrow), blood capillary with pericyte (B) and a neutrophil (N) in the propria-submucosa. x 830; (bar 2 µm).

Figure 15: TEM of the LT showing high endothelial venule (HV) and a neutrophil (N) in the propria-submucosa. Note the electron-dense granules (arrow) in the cytoplasm. x 2100; (bar 1 µm).

towards the nuclear membrane. These nuclei generally contained one eccentric nucleolus. The cytoplasm of these cells was electron-lucent and contained few organelles like mitochondria, endoplasmic reticulum, and Golgi apparatus. The luminal surface of these cells possessed small microvilli-like processes (Figure **16**). The cytoplasm of these cells also contained small vacuoles which were considered equivalent to those of vesiculo-vacuolar organelles (VVO's) (Figures **17** and **18**). These VVO's were mainly observed in the processes of these endothelial cells projecting into the lumen. Besides, the cytoplasm also presented some granules, membrane-bound bodies, vacuolated structures (Figure **18**). The adjacent endothelial cells were attached by desmosomes. At some places, the lymphocytes traversing through transendothelial or inter-endothelial routes also observed.

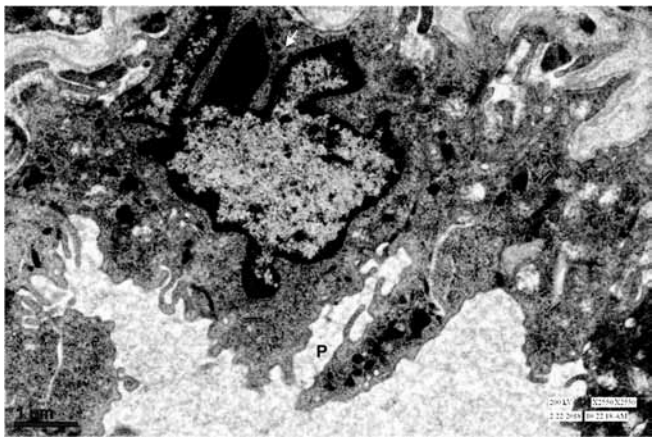

Figure 16: TEM of the high endothelial venule showing nuclear indentation (arrow) and cytoplasmic processes (P) of the endothelial cell. x 2550; (bar 1 µm).

Figure 17: TEM of the endothelial cell of a high endothelial venule showing granules, membrane bound bodies (D), and vesiculo-vacuolar organelles (V). x 7000; (bar 0.5 µm).

DISCUSSION

The surface of the lingual tonsil revealed a highly irregular mucosa with folds oriented in different directions, separated by shallow depressions or the

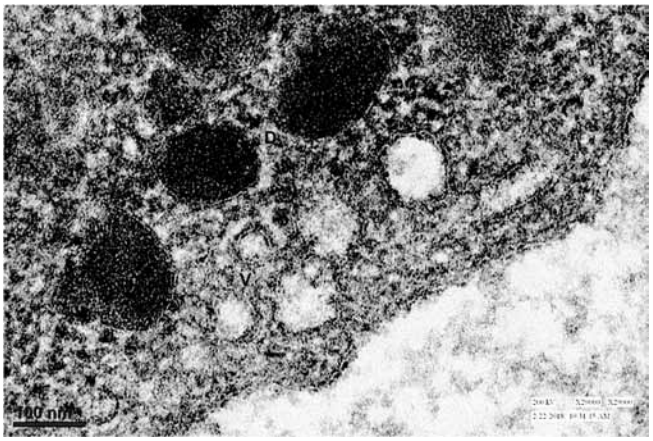

Figure 18: TEM of the endothelial cell of a high endothelial venule at a higher magnification showing granules (arrow), membrane bound bodies (D), vacuolated structures and vesiculo-vacuolar organelles (V). x 29000; (bar 100 nm).

grooves as reported in the horse [1]. In the pig, the irregular surface presented papillae of varying shapes and size [8]. The higher magnification presented the squamous arrangement of cells delineated from the adjacent cells, similar to that of the goat [9]. In the horse, the flat squamous epithelial cells formed a sheath-like structure [1]. The desquamating cells observed as previously reported in the horse [1] and goat [9].

Similarly, variable patterns of microplicae observed with an additional magnification of the cell surface. These microplicae were frequently of closed pattern type and resembled those fingerprints of human beings as reported in the horse [1], goat [9, 10] and the pig [8]. The microplicae of the adjacent cells were independent of each other and usually had thicker arrangement at the junction of the two cells as described in the goat [9], ovine [11] and the pig [8]. At sites of desquamation, the microplicae of underlying and superficial cells were merged in the horse [1]. The surface of the tonsil also presented different patterns of small openings of glandular ducts as reported in the horse [1] and goat [9]. These openings identified as the orifices of the crypts of the tonsillar follicles [12]. These duct-like structures usually had a narrow rim having the cells arranged in an overlapping pattern. The microplicae were not distinct in the cells lining the lumen of the ducts; however, small microvilli like arrangements also observed.

The different features of the epithelium described in light microscopy [7] were confirmed by transmission electron microscopy. The elongated nuclei of the stratum basale contained clumps of electron-dense chromatin material which was irregularly distributed whereas, in the horse, the chromatin mainly localized toward the outer nuclear membrane [1]. The cytoplasm presented the cell organelles, which in the horse was rich in uniformly distributed polyribosomes [1]. The intercellular spaces presented small microvilli-like projections of the cells. In the horse, the cell membrane abutted on the undulating basal lamina in the form of small-blunted pedicles [1]. The electron-lucent nuclei of stratum spinosum were irregularly shaped; however, these were elongated in the horse [1] and both of which contained centric/eccentric one-two nucleoli. The cytoplasm of these cells contained several tonofilaments, as reported in the horse [1]. These cells were also attached by several desmosomes, and their interdigitating villi were very closely associated with each other, as observed in the horse [1]. The stratum granulosum had horizontally oriented electron-lucent nuclei with one centric nucleolus. Their cytoplasm had few filaments, cell organelles and few membrane-bound organelles. These cells possessed large processes which were tapering, and the intercellular spaces presented interdigitating villi-like projections.

The cells of the stratum corneum were either devoid or had degenerating nuclei, and cell organelles were lacking as observed in the stratum superficiale of the horse [1]. The free surface of these cells presented small spicule-like projections and the desquamating cells. In the horse, the cells of the stratum superficiale presented small irregular blunt or spiny microvilli, which were attached to those of adjacent cells by numerous desmosomes [1]. The upper epithelial layers were well keratinized and contained small apical protrusions in the ovine [11].

The reticular epithelium having stratified squamous non-keratinized epithelium characterized by massive infiltration of lymphoid cells from the underlying lymphoid tissue. The features of strata basale and spinosum resembled those of the surface epithelium as reported in the horse [1]. The stratum superficiale presented the different types of surface epithelial cells, which were a cuboidal or squamous type. Their electron-lucent nuclei presented smaller clumps of chromatin towards the nuclear membrane as observed in the horse [1]. The free surface of these cells presented microscopic-sized microvilli-like projections.

The propria-submucosa presented the fine blood capillaries, reticular cells, fibroblast, lymphoid cells and collagen bundles as described in the light microscopy [7]. Moreover, stellate shaped follicular dendritic cells (FDC) with delicate branching cytoplasmic processes

and a few macrophages and plasma cells also observed in the buffalo calf [6] and horse [1]. FDC developed through the transformation of fibroblastic reticulum cells during germinal centre formation [13]. However, the desmosomal attachment of their processes suggested an epithelial rather than mesenchymal origin. The existence of these cells and their accumulation in the primary follicles depend on the presence of B cells [14]. Integrins are key factors that support interactions of B-cells with FDCs [15]. Thus, B-cells depleted animals, or mice compounded with severe immunodeficiency lacked follicular aggregates of FDCs [16]. FDC bind antigen-antibody complexes to their surface for long periods and are essential for the generation of effective humoral antibody responses [17]. Similarly, a few mast cells with irregular nuclei and electron-dense chromatin material observed in its deeper part, especially in the vicinity of blood capillaries in the horse [1].

A few high endothelial venules interspersed in the lymphoid tissues observed as earlier described in the light microscopy [7]. The high endothelial venules (HEVs), an integral component of the mucosa-associated lymphoid tissue, were specialized vessels that supported active lymphocyte migration from peripheral blood to secondary lymphoid organs [18; 4]. The constitutive trafficking of naive lymphocytes in and out of lymphoid organs was a prerequisite for the detection of processed antigen on mature dendritic cells and the initiation of immune responses [19]. Although lymphocyte migration from HEVs did not depend on exogenous inflammatory stimuli, it had features in common with the migration of leukocytes to inflammatory sites [20]. The nuclei of these endothelial cells were irregular in shape as reported in the horse [4] whereas, in the buffalo calf, these were polyhedral shaped [6].

The cytoplasm of these endothelial cells was electron-dense and contained cell organelles such as mitochondria, endoplasmic reticulum, Golgi apparatus and small vacuoles which were considered equivalent to vesiculo-vacuolar organelles (VVOs). These were in agreement with findings in the horse [4] and the buffalo calf [6]. The VVOs described as new endothelial cell organelles that provided a significant mode of extravasation of macromolecules at sites of augmented vascular permeability induced by vascular permeability factor/vascular endothelial growth factor (VPF/VEGF), cytokine [21], associated with venules of experimental tumours [22, 23]. The microvilli-like small processes on the luminal surface of the endothelial cells observed in the present study were variable in the horse ranging from smooth to filiform or microvillus and sometimes branching. Additionally, the lumen contained filaments and vesicles, along with a few multivesicular bodies, as seen in the horse [4].

CONCLUSION

The SEM of the lingual tonsil revealed the irregular mucosal folds, having a squamous arrangement of cells presenting the microplicae of varying patterns. The glandular ducts openings were of different shapes. The TEM demonstrated the cellular details of the distinct strata of the different epithelia. The cytoplasmic process of the cells of high endothelial venules consisted of some membrane-bound granules, membrane bound bodies and small vacuoles which were considered vesiculo-vacuolar organelles.

ACKNOWLEDGEMENTS

The authors sincerely acknowledged the Indian Council for Cultural Relation ICCR for the international PhD fellowship offered to Dr Ibrahim Alhaji Girgiri. The facility provided by EM Lab., AIIMS and AIRF, JNU, New Delhi, India was duly acknowledged.

CONFLICT OF INTEREST

The authors do not have any conflict of interest.

FUNDING STATEMENT

The authors did not get any funding for the present research work.

REFERENCES

[1] Kumar P, Timoney JF. Histology and ultrastructure of the equine lingual tonsil. I. crypt epithelium and associated structures. Anat Histol Embryol 2005; 34: 27-33. https://doi.org/10.1111/j.1439-0264.2004.00560.x

[2] Brandtzaeg P. Immunology of tonsils and adenoids: everything the ENT surgeon needs to know. Int J Pediatr Otorhinolaryngol 2003; 67S1: 69-76. https://doi.org/10.1016/j.ijporl.2003.08.018

[3] Brandtzaeg P, Pabst P. Let's go mucosal: communication on slippery ground. Trends Immunol 2004; 25: 570-78. https://doi.org/10.1016/j.it.2004.09.005

[4] Kumar P, Timoney JF. Histology and ultrastructure of the equine lingual tonsil. II. lymphoid tissue and associated high endothelial venules. Anat Histol Embryol 2005; 34: 98-104. https://doi.org/10.1111/j.1439-0264.2004.00579.x

[5] Horter DC, Yoon JK, Zimmerman JJ. A review of porcine tonsils in immunity and disease. Anim Health Res Rev 2003; 4(2): 143-55. https://doi.org/10.1079/AHRR200358

[6] Ez Elarab SM, Zidan M, Zaghloul MD, Derbalah AE. Histological structure of the lingual tonsils of the buffalo calf (Bos Bubalus). Alexandria J Vet Sci 2016; 49(1): 78-84. https://doi.org/10.5455/ajvs.222704

[7] Girgri IA, Kumar Pawan. Histological and histochemical studies on the lingual tonsil of the buffalo (Bubalus bubalis). J Buff Sci 2019; 8: 68-76. https://doi.org/10.6000/1927-520X.2019.08.03.3

[8] Ranjit Kumar P, Kumar P, Singh G. Histology, histochemistry and scanning electron microscopy of lingual tonsil of the young pigs. Vet Res Int 2015; 3(1): 55-9.

[9] Kumar P, Kumar P. Light and scanning transmission electron microscopic studies on lingual tonsil of goat. Haryana Vet 2005; 44: 13-6.

[10] Indu VR, Lucy KM, Ashok N, Maya S. Histology and scanning electron microscopy of the tubal tonsil of goats. Int J Current Microbiol App Sci 2015; 6 (3): 1716-22. https://doi.org/10.14202/vetworld.2015.1011-1014

[11] Casteleyn C, Cornelissen M, Simoens P, Van den Broeck W. Ultramicroscopic examination of the ovine tonsillar epithelia. Anat Rec 2010; 293: 879-89. https://doi.org/10.1002/ar.21098

[12] Cocquyt G, Simoens P, Muylle S, Van den Broeck W. Anatomical localization and histology of bovine tonsils. Res Vet Sci 2008; 83: 166-73. https://doi.org/10.1016/j.rvsc.2007.04.011

[13] Heusermann U, Zurborn KH, Schroeder L, Stutte HJ. The origin of the dendritic reticulum cell. An experimental enzyme histochemical and electron microscopic study on the rabbit spleen. Cell Tissue Res 1980; 209: 279-94. https://doi.org/10.1007/BF00237632

[14] Brandtzaeg P. Immunobiology of the tonsils and adenoids. Mucosal Immunol 2015; 2: 1985-2016. https://doi.org/10.1016/B978-0-12-415847-4.00103-8

[15] Wang X, Rodda LB, Bannard O, Cyster JG. Integrin-mediated interactions between B cell and follicular dendritic cells influence germinal centre B cell fitness. J Immunol 2014; 192: 4601-09. https://doi.org/10.4049/jimmunol.1400090

[16] MacLennan ICM. Germinal centres. Annu Rev Immunol 1994; 12: 117-39. https://doi.org/10.1146/annurev.iy.12.040194.001001

[17] Heinen E, Bosselloir A, Bouzahzah F. Follicular dendritic cells. Origin and function. Curr Top Microbiol Immunol 1995; 201: 15-47. https://doi.org/10.1007/978-3-642-79603-6_2

[18] Zidan M, Jecker P, Pabst R. Differences in lymphocyte subsets in the wall of high endothelial venules and the lymphatics of human palatine tonsils. Scand J Immunol 2000; 51: 372-76. https://doi.org/10.1046/j.1365-3083.2000.00681.x

[19] Butcher EC, Picker LJ. Lymphocyte homing and homeostasis. Sci 1996; 272: 60-6. https://doi.org/10.1126/science.272.5258.60

[20] Christelle F, Graham P, Ann A. Transendothelial migration of lymphocytes across high endothelial venules into lymph nodes is affected by metalloproteinases. Blood 2001; 98: 688-95. https://doi.org/10.1182/blood.V98.3.688

[21] Dvorak AM, Feng D. The vesiculo-vacuolar organelle (VVO): a new endothelial cell permeability organelle. J Histochem Cytochem 2001; 49: 419-31. https://doi.org/10.1177/002215540104900401

[22] Kohn S, Nagy JA, Dvorak HF, Dvorak AM. Pathways of macromolecular tracer transport across venules and small veins. Structural basis for the hyperpermeability of tumor blood vessels. Lab Invest 1992; 67: 596-607.

[23] Dvorak HF, Nagy JA, Feng D, Brown LF, Dvorak AM. The vesiculo-vacuolar organelle (VVO): a distinct endothelial cell structure that provides a transcellular pathway for macromolecular extravasation. J Leukoc Biol 1996; 59: 100-15. https://doi.org/10.1002/jlb.59.1.100

Received on 06-01-2020 Accepted on 06-02-2020 Published on 11-02-2020

DOI: https://doi.org/10.6000/1927-520X.2020.09.02